Laboratory Investigation (2005) 85, 436–446

www.laboratoryinvestigation.org

Alterations of DNA damage-response genes *ATM* and *ATR* in pyothorax-associated lymphoma

Angen Liu[1], Tetsuya Takakuwa[1], Shigeki Fujita[1], Maria Francisca Ham[1], Wen-Juan Luo[1], Masanori Daibata[2] and Katsuyuki Aozasa[1]

[1]*Department of Pathology, Osaka University Graduate School of Medicine, Osaka, Japan and* [2]*Department of Hematology and Respiratory Medicine, Kochi Medical School, Kochi University, Kochi, Japan*

Pyothorax-associated lymphoma (PAL) is non-Hodgkin's lymphoma that develops from chronic inflammation. Free radicals and oxidative stress generated in the inflammatory lesions could cause DNA damage and thus provide a basis for lymphomagenesis. Ataxia-telangiectasia mutated (*ATM*) and *ATM* and Rad3-related (*ATR*) genes are responsive genes for DNA damage, therefore potential involvement of these genes in PAL lymphomagenesis was examined in eight PAL cell lines and clinical samples from five cases. *ATM* mutations were detected in five of eight PAL lines. All but one of these mutations affected the phosphatidylinositol 3-kinase domain, indicating the loss-of-function mutation of *ATM* gene. Heterozygous mutations of *ATR* were found in two of eight lines; one a missense and the other a truncation mutation. *ATR* mutations were also detected in two of five cases in clinical samples from PAL. PAL cells with *ATR* mutation showed a delay or abrogation in repair for ionizing radiation (IR)-induced DNA double-strand breaks (DSBs) or ultraviolet (UV)-induced DNA single-strand breaks (SSBs), and exhibited a defect in p53 accumulation and failure in cell cycle checkpoint at G1–S phase. These findings showed that mutations of *ATR* gene result in failure for DNA DSB and SSB repair, suggesting the role of *ATM* and *ATR* gene mutations in PAL lymphomagenesis.
Laboratory Investigation (2005) **85,** 436–446, advance online publication, 31 January 2005; doi:10.1038/labinvest.3700235

Keywords: DNA repair; *ATM*; *ATR*; pyothorax-associated lymphoma; cell lines

There is general agreement on the role of chronic inflammation in tumorigenesis, in which DNA-damage-promoting agents are considered to potentiate neoplastic risk.[1] Malignant lymphoma frequently develops in the pleural cavity of patients with over 20-year histories of pyothorax, and the term pyothorax-associated lymphoma (PAL) has been proposed for this type of tumor.[2,3] Most PALs are diffuse large cell lymphomas of B-cell type, whereas unusual types of PAL have also been reported,[2] indicating the unique etiology of PAL, that is, malignant lymphoma developing in long-standing inflammation. Until now, at least eight cell lines derived from PAL tissues have been established.[4–7] These lines could be used for studying the effect of chronic inflammation in lymphomagenesis.

Correspondence: Dr T Takakuwa MD, Department of Pathology (C3), Osaka University Medical School, 2-2 Yamada-oka, Suita, Osaka 565-0871, Japan.
E-mail: takakuwa@molpath.med.osaka-u.ac.jp
Received 11 September 2004; revised 9 November 2004; accepted 16 November 2004; published online 31 January 2005

Maintenance of genome stability partly depends on the proper regulation of cellular responses to DNA damage and the integrity of the DNA repair system.[8] Disruption of this system might result in cancer. In mammalian cells, two members of the phosphatidylinositol 3-kinase-related kinase (PI3KK) family, ataxia-telangiectasia mutated (*ATM*) and *ATM* and Rad3-related (*ATR*) kinases play a central role in DNA damage recognition and the initial phosphorylation events.[9–12]

The *ATM* protein engages in multiple biochemical pathways, linking recognition and repair of DNA double-strand breaks (DSBs) to downstream cellular processes, such as delay or arrest of cell cycle and accelerated programmed cell death.[8] *ATM* is exclusively responsive to DNA DSBs, and plays an important role in the development of lymphoid cells in which DSBs occur frequently in physiological conditions. Patients with inactivated *ATM* gene on both alleles are vulnerable and hypersensitive to agents causing DNA DSBs, and thus highly predispose to the development of leukemia and lymphoma.[11] Chromosomal translocations involving T-cell receptor (TCR) genes are frequent in these

patients, and T-cell malignancies are prone to develop. *ATM* alterations are also believed to be involved in the pathogenesis of sporadic T-prolymphocytic leukemia (T-PLL)[13–15] and sporadic B-cell chronic lymphocytic leukemia (B-CLL).[16–18]

ATR is essential for cell proliferation; *ATR*-deficient mice die early in embryonic life.[19,20] Since *ATR* null cell lines are not available, functional analysis of this gene *in vitro* is limited. Overexpression of a dominant-negative construct or *cre-lox*-mediated gene loss has been a mainstay in research of *ATR* function.[21] Previous studies have suggested that ATR also may participate in the signaling of ionizing radiation (IR)- and ultraviolet (UV)-induced DNA damage.[9,10,22] Recently, O'Driscoll *et al*[23] reported that a splicing mutation affecting expression of *ATR* results in Seckel syndrome, an autosomal recessive disorder that shares features with disorders showing impaired DNA-damage responses, such as Nijmegen breakage syndrome. A fibroblast cell line derived from a patient with Seckel syndrome shows impaired response to DNA damage induced by UV and mitomycin C, suggesting that UV-induced *ATR* activation can occur through nucleotide excision repair. Recent studies showed that *ATR* gene plays a role in maintenance of stability in fragile sites, that is, decreased expression of the *ATR* resulted in the breakage of these sites.[24]

To analyze the role of *ATM* and *ATR* gene alterations in the lymphomagenesis of PAL, mutations of these two genes were examined in the PAL cell lines. Two cell lines with heterozygous mutations in *ATR* gene were further analyzed to evaluate their functional consequence in repair of IR-induced DNA DSB and UV-induced DNA single-strand break (SSB) and cell cycle regulations.

Materials and methods

Cell Lines

PAL cell lines used were OPL-1, OPL-2, OPL-3, OPL-4, OPL-5, OPL-7, Pal-1, and Deglis.[4–7] Characteristics of these eight lines are summarized in Table 1. These lines were established from eight patients with PAL, with a 39–66 year history of chronic pyothorax resulting from artificial pneumothorax for the treatment of pulmonary tuberculosis or tuberculous pleuritis. Deglis was a kind gift from Dr Al Saati.[7] One Ataxia-Telangiectasia cell line (AT(L)5KY), one lymphoblastoid cell line (IB4), and a total of eight leukemia-lymphoma cell lines derived from Burkitt lymphoma (BL36, BL60, BL137, Namalwa, Raji) and adult T-cell leukemia (MT-1, MT-2, MT-4) were used as controls. AT(L)5KY, Namalwa and Raji were obtained from Japanese Collection of Research Bioresources (Tokyo, Japan). Other cell lines were the generous gifts from investigators listed in Acknowledgments. All cell lines were incubated in RPMI1640 medium (Sigma, St Louis, MO, USA) supplemented with 10% heat-inactivated fetal bovine serum and antibiotics at 37°C in a humidified atmosphere of 5% CO_2 and 95% air.

Patients

Clinical samples from five patients with PAL who were admitted to hospitals in Osaka, Japan during the period from 1994 to 1999 were included for the analysis. Age of the patients at first admission for PAL ranged from 63 to 75 (median, 73.0) years, with a male to female ratio of 4:1. Histologic specimens obtained by biopsy were fixed in 10% formalin and routinely processed for paraffin embedding, or snap frozen for extraction of total RNA. Histologic sections cut at 4 μm were stained with hematoxylin and eosin and by an immunoperoxidase procedure. All tumors were histologically classified according to the World Health Organization classification as diffuse large B-cell lymphoma.

Isolation of DNA and Total RNA, RT-PCR, and Detection of Mutations

DNA and/or total RNA were extracted from the cell lines and clinical materials with the TRIzol reagent (Invitrogen, Inc., Rockville, MD, USA) according to the manufacturer's instructions. In all, 5 μg of total

Table 1 Summary of characteristics of PAL cell lines

Cell lines	*Age (years)*	*Sex*	*Duration of pyothorax (years)*	*Immunophenotype*						*EBV status*			*References*
				CD2	*CD3*	*CD7*	*CD10*	*CD19*	*CD20*	*LMP-1*	*EBNA2*	*EBERs ISH*	
OPL-1	76	M	46	ND	−	ND	−	−	+	−	+	ND	Kanno *et al*[4]
OPL-2	67	M	40	ND	ND	ND	−	−	+	−	−	ND	Kanno *et al*[4]
OPL-3	72	M	51	+	−	−	−	−	+	+	+	+	Takakuwa *et al*[5]
OPL-4	82	F	63	−	−	−	−	−	+	−	−	+	Takakuwa *et al*[5]
OPL-5	74	F	66	−	−	−	−	−	+	+	−	+	Takakuwa *et al*[5]
OPL-7	74	F	54	−	−	−	−	+	+	−	+	+	Takakuwa *et al*[5]
Pal-1	68	M	40	+	−	−	−	−	+	+	+	+	Daibata *et al*[6]
Deglis	68	M	39	+	+	+	−	+	+	+	+	ND	Al Saati *et al*[7]

ND indicates not done.

RNA were reverse-transcribed by random hexamer priming using the superscript first strand synthesis system (Invitrogen).

Seminested RT-PCR was performed to amplify the *ATM* and *ATR* transcripts using five sets and four sets of primers, respectively, spanning the whole open reading frame in PAL cell lines (Table 2). After electrophoresis on 1.0% agarose gels, DNA fragments were excised and purified using the Wizard SV gel extraction kit (Promega, Madison, WI, USA). DNA was directly sequenced using the purified DNA fragments as template and appropriate primers. When the potential mutations were suspected, the same PCR reactions were reperformed, followed by cloning of the products into the plasmid pCR2.1-TOPO (Invitrogen), and then eight to 10 clones were sequenced to conform to the mutations.

Cell Cycle Analysis Using Flow Cytometry (FCM)

FCM analysis was performed based on the methods described previously.[25] In brief, cells were exposed to either 2 Gy of IR or 10 J/m^2 of UV light and incubated for 18 h. Cells without IR or UV treatment were used as control. After staining with propidium iodide, samples were analyzed with FCM. Data were collected and analyzed with the Cell Quest DNA quantitation program (Becton Dickinson).

Expression of p53 by Western Blotting

Cells were counted using Sysmex (Sysmex, KX-21, Kobe, Japan) and equal numbers of cells were exposed to 10 Gy of IR and 50 J/m^2 of UV light, respectively, and incubated for up to 6 h. Whole cells were lysed by sonication in a buffer containing 15 mM Tris-HCl (pH 6.8), 10% glycerol, 2% SDS, and 6% β-mercaptoethanol. Following incubation at 95°C for 10 min, equal volume of protein extracts was separated by 10% SDS-PAGE, and blotted to a PVDF membrane using a wet-blotting apparatus. Blots were blocked in PBS containing 0.05% Tween 20 and 1% nonfat dry milk, and incubated with anti-p53 antibody (DakoCytomation, Glostrup, Denmark) and anti-β-actin (Sigma-Aldrich, Steinheim, Germany) as control at room temperature for 1 h. Signals were visualized with ECLplus chemiluminiscent reagents (Amersham Pharmacia Biotech, UK).

Table 2 Oligonucleotide primers used for PCR reactions

	1st primer sequence	*2nd primer sequence*	*PCR products (bp)*[a]
cDNA primers			
ATM1	F 5′-CTGCTGCCCAGATATGACTTC-3′ R 5′-AGAAGACAGCGATCCAGTG-3′	5′-CAGTGATGTGTGTTCTGAAATTGTG-3′ 5′-AGAAGACAGCGATCCAGTG-3′	2113 (nt. 161–2273)[b]
ATM2	F 5′-GTTACGATGCCTTACG-3′ R 5′-CAGTAATAAACTAACAAACAGGTG-3′	5′-GGCTTCTCTGTCCACCAG-3′ 5′-CAGTAATAAACTAACAAACAGGTG-3′	2316 (nt. 2224–4539)
ATM3	F 5′-AGAACCTCACCTTGTG-3′ R 5′-CCAGCCAGAAAGCATC-3′	5′-CAAATAATGTTTATAAGAAGCACAG-3′ 5′-CCAGCCAGAAAGCATC-3′	1518 (nt. 4475–5992)
ATM4	F 5′-GCCTGGATGATATAAATC-3′ R 5′-CCTCCCATCATCTTGGTCC-3′	5′-GCTTGCTGTTGTGGAC-3′ 5′-CCTCCCATCATCTTGGTCC-3′	1875 (nt. 5916–7790)
ATM5	F 5′-GATGAAGAGAGACGGAATGAAG-3′ R 5′-GTATGTTGGCAGGTTAAAAATAAAGGCT-3′	5′-GATGAAGAGAGACGGAATGAAG-3′ 5′-GGCTGAATGAAAGGGTAATTCATATAC-3′	1696 (nt. 7698–9393)
ATR1	F 5′-GGAGACGCCGGGAAC-3′ R 5′-GAATCTTGGGAACTCTGTTAC-3′	5′-CGTTGGCGTGGTTGAC-3′ 5′-GAATCTTGGGAACTCTGTTAC-3′	2109 (nt. 70–2179)
ATR2	F 5′-GCACTGAAACAGAAAGCTGA-3′ R 5′-CAGAGCAACCGAGCTTG-3′	5′-GTGGAGAACAGCAGTTTAC-3′ 5′-CAGAGCAACCGAGCTTG-3′	2112 (nt. 2055–4166)
ATR3	F 5′-ATCACCTGAACTGATGGCT-3′ R 5′-CGGCCCACTAGTAGCAT-3′	5′-CTGATAAAGTATGCAACAGAC-3′ 5′-CGGCCCACTAGTAGCAT-3′	2072 (nt. 4057–6128)
ATR4	F 5′-CACCAGGCACTAATTGTTC-3′ R 5′-CAACCACAGATTCATACC-3′	5′-CACCAGGCACTAATTGTTC-3′ 5′-GCATTACTTTTAGATTATTAACAT-3′	2073 (nt. 6013–8085)
Genomic primers			
ATMexon8	F 5′-AAATCCTTTTTCTGTATGGGAT-3′		350
ATMexon8	R 5′-GTTACTGAGTCTAAAACATGG-3′		
ATMexon33	F 5′-ATTACAGTAAGTTTTGTTGGCT-3′		317
ATMexon33	R 5′-GCTAGAGCATTACAGATTTTTG-3′		
ATMexon34	F 5′-CAGTGTCTATAAATGGCAC-3′		324
ATMexon34	R 5′-GTGACAATGAAACCAAGAG-3′		
ATMintron61	F 5′-ATTTAATAATGAAGCTGGTTTGG-3′		396
ATMintron61	R 5′-CCTCTAGGATTGATTACTTG-3′		
ATMexon62	F 5′-TAAAGTTCACATTCTAACTGG-3′		267
ATMexon62	R 5′-GGTGCAAAGAACCATGC-3′		
ATRexon46	F 5′-GCTGCTGTCTTCTTTCACTTGTGACA-3′		333
ATRexon46	R 5′-CACCTTCATTCCCCGTAGTTCTTTCA-3′		

[a]Range of nucleotides in parentheses.
[b]nt. Indicates nucleotide.
Accession number of ATM: NM000051; ATR: NM001184.

DNA Double-Strand Break (DSB) Repair Assays

More than 1×10^5 cells from each cell line were embedded in agarose plugs as described previously.[26] The plugs on ice were exposed to 20 Gy of IR, covered with RPMI1640 medium, and kept at 37°C for up to 6 h to allow the cells to repair damaged DNA. Untreated plugs containing the same concentration of cells were used as control. The plugs were embedded into wells of a 0.8% agarose gel in 1 × TAE, and subjected to pulsed-field gel electrophoresis (PFGE) in a CHEF apparatus (Bio-Rad, Hercules, CA, USA) at 3 V/cm at 14°C for 48 h with a pulse time of 45 s. Under these PFGE conditions, DNA fragments between 2 and 6 megabases migrate as a single band and form a compression zone under each well, whereas most rejoined DSB would be too large to enter the gel. After electrophoresis, DNA was stained with ethidium bromide and visualized with UV light. The signals from the wells and compression zones were measured using FMBIO Analysis V8.0 (TaKaRa, Kusatsu, Japan). DSBs were quantified as the fraction of DNA in the compression zone relative to that in the wells.

DNA Single-Strand Break (SSB) Repair Assays

To evaluate DNA single-strand break repair, alkaline single cell gel electrophoresis (Comet assay) was performed as previously described with some modifications.[27,28] Briefly, more than 5×10^3 cells were mixed with 50 μl of 0.5% low melting point agarose in 1 × PBS at 37°C. The cell mixture was layered onto a microscope slide previously coated with 80 μl of 0.65% normal agarose in PBS, and then exposed to 10 J/m^2 of UV. After UV exposure, a top layer of 80 μl of low melting point agarose was added, and incubated for up to 18 h in the medium at 37°C. Thereafter, the slides were put into the lysis solution (2.5 M NaCl, 10 mM Tris-HCl, 100 mM EDTA and 1% Triton X-100, pH 10) at 4°C for 1 h, and incubated in the electrophoretic buffer (1 mM EDTA, 300 mM NaOH, pH 13) at 4°C for 40–60 min to allow unwinding of DNA. After electrophoresis for 40 min at constant current of 300 mA, the slides were washed in neutralization buffer (0.4 M Tris-HCl, pH 7.5), and stained with ethidium bromide. In all, 50 cells were analyzed based on the methods for collecting comet data, in which repair of DNA SSBs was quantified and defined as the 'DNA migration length (DML)', a ratio of the comet length to its width.

Statistical Analysis

Comparisons were made using Student's *t*-test (unpaired): *P*-value less than 0.05. taken as statistically significant.

Results

Mutation Analysis of PAL Cell Lines

ATM *gene*

Mutations of *ATM* gene were detected in five of eight PAL lines: four frameshifts in three lines and two missense mutations in two (Table 3). Missense mutations involved codons 213 (TTT→GTT; Phe→Val) and 2974 (CCG→CTG; Pro→Leu) in OPL-1 and Pal-1, respectively (Gene Bank accession number NM000051). In Pal-1, missense mutation affected the phosphatidylinositol-3 kinase (PI3K) domain of the *ATM* protein.

In OPL-3, 22 bps deletion was found in exon 8. In OPL-4, deletion of exons 33 and 34 plus 9 bps insertion between exons 37 and 38, and deletion of exon 62 plus 72 bps insertion between exons 61 and 63 were found. In OPL-5, deletion of exon 34 was

Table 3 *ATM* and *ATR* mutations in PAL cell lines

Cell lines	ATM			ATR		
	Nucleotide change	*Predicted effect*	*Frequency of mutation-positive clones (%)*	*Nucleotide change*	*Predicted effect*	*Frequency of mutation-positive clones (%)*
OPL-1	T826G	Phe→Val	50	WT	—	—
OPL-2	WT	—	—	Exon 46/47 ins 137 bp	Frameshift	40
OPL-3	Exon 8 del 22 bp	Frameshift	67	WT	—	—
OPL-4	Del exon 33, 34+exon 37/38 ins 9 bp	Frameshift	60	WT	—	—
	Del exon 62+ins 72 bp	Frameshift	33			
OPL-5	Del exon 34	Frameshift	33	WT	—	—
OPL-7	WT	—	—	WT	—	—
Deglis	WT	—	—	WT	—	—
Pal-1	C9110T	Pro→Leu	60	T7637C	Val→Ala	25

WT indicates wild type.

found. All of the frameshift mutations were heterozygous and generating an in-frame stop codon, which resulted in the deletion of PI3K domain. In these three lines, sequences around the skipped exon and inserted nucleotides were analyzed. In OPL-3, 2 bps shortening of poly (T) 15 repeat within *ATM* intron 7 was identified. In other cell lines, no mutations were detected in the sequences around the skipped exon and inserted nucleotides examined (data not shown).

ATR *gene*

Missense mutation was found in exon 45 of the Pal-1, which affected codon 2511 (GTG→GCG; Val→Ala) (Gene Bank accession number NM001184). In OPL-2, an insertion of 137 bp from intron 46 was found between exons 46 and 47 (Table 3). This mutation was heterozygous and generated an in-frame stop codon. The mutation in the acceptor–donor splice site, or around the insertion sequences of *ATR* intron 46 might generate an aberrant insertion between exons 46 and 47 in OPL-2. To examine this hypothesis, genomic DNA from OPL-2 was amplified using primer pairs flanking exon 46, 47 and the insertion sequences. However, the expected mutations could not be detected (data not shown). To exclude the possibility of a rare polymorphism, mutations of *ATR* in Pal-1 and OPL-2 were searched for in one lymphoblastoid cell line (IB4) and a series of leukemia–lymphoma cell lines, BL36, BL60, BL137, Namalwa, Raji, MT-1, MT-2, MT-4. However, the same mutations could not be found.

Polymorphisms and Alternative Splicing within ATR Gene

Dinucleotide and single nucleotide changes were observed at one and five loci of *ATR* gene, respectively (Table 4). Polymorphisms of dinucleotide change CG→GC at nucleotides 379–380 and single nucleotide change A→G at nucleotide 7980 have already been reported.[29] Other single nucleotide changes including T737C, T1881A, T1920C, and T5313C were observed in more than half of PAL lines, indicating that these changes were also polymorphisms rather than mutations. Nucleotide changes at 379–380 and 737 result in amino-acid alterations, Arg→Ala and Met→Thr, respectively, while other nucleotide changes do not result in amino-acid changes.

Skipping of exon 6, reported to be due to alternative splicing,[30] was detected in Pal-1 and Deglis.

Mutation Analysis of Clinical Samples

Mutations of *ATM* and *ATR* gene coding PI3K domain were examined on clinical samples. *ATR* gene mutations were detected in two of five cases (Figure 1). An insertion of 137 bp from intron 46 between exons 46 and 47, the same mutations as observed in OPL-2 line, was found in one case. A deletion from nucleotide 6184–7297, which correspond to exons 36–42, was found in another case. Both mutations were heterozygous and generated an in-frame stop codon. *ATM* transcripts could be amplified in three of five cases, in which mutations were not detected (data not shown).

Functional Consequence of ATR Mutation

To assess the functional consequence of *ATR* mutation for DNA-damage response and cell cycle regulation, the characteristics of Pal-1, which carries both *ATM* and *ATR* heterozygous missense mutations, and OPL-2, which carries heterozygous *ATR* mutation, were subjected to the following studies. OPL-7 and one lymphoblastoid cell line (IB4), which carries no mutation within ATM, ATR and p53, were used as negative control, and one AT(L)5KY was used as positive control.

Table 4 Polymorphisms and alternative splicing in *ATR* gene

Cell lines	*Nucleotide sites*						*Alternative splicing Del exon 6*
	379, 380[a] *CGC→GCC (Arg→Ala)*[b]	*737 ATG→ACG (Met→Thr)*[b]	*1881 GGT→GGA (Gly→Gly)*[b]	*1920 GAT→GAC (Asp→Asp)*[b]	*5313 TAT→TAC (Tyr→Tyr)*[b]	*7980*[a] *CAA→CAG (Gln→Gln)*[b]	
OPL-1	GC	C	A	C	C	A	–
OPL-2	GC	C/T	A	C	C/T	G	–
OPL-3	GC	T	T	T	T	G/A	–
OPL-4	GC	C/T	A/T	C	T	A	–
OPL-5	GC	C/T	A/T	T	T	G/A	–
OPL-7	GC	T	T	T	T	A	–
Pal-1	CG	C/T	A	C/T	C/T	A	+
Deglis	CG	C	A	T	C/T	A	+

[a]Reported polymorphism (GenBank accession number U49844).
[b]Amino-acid changes generated by nucleotide changes at indicated sites are shown in parentheses.

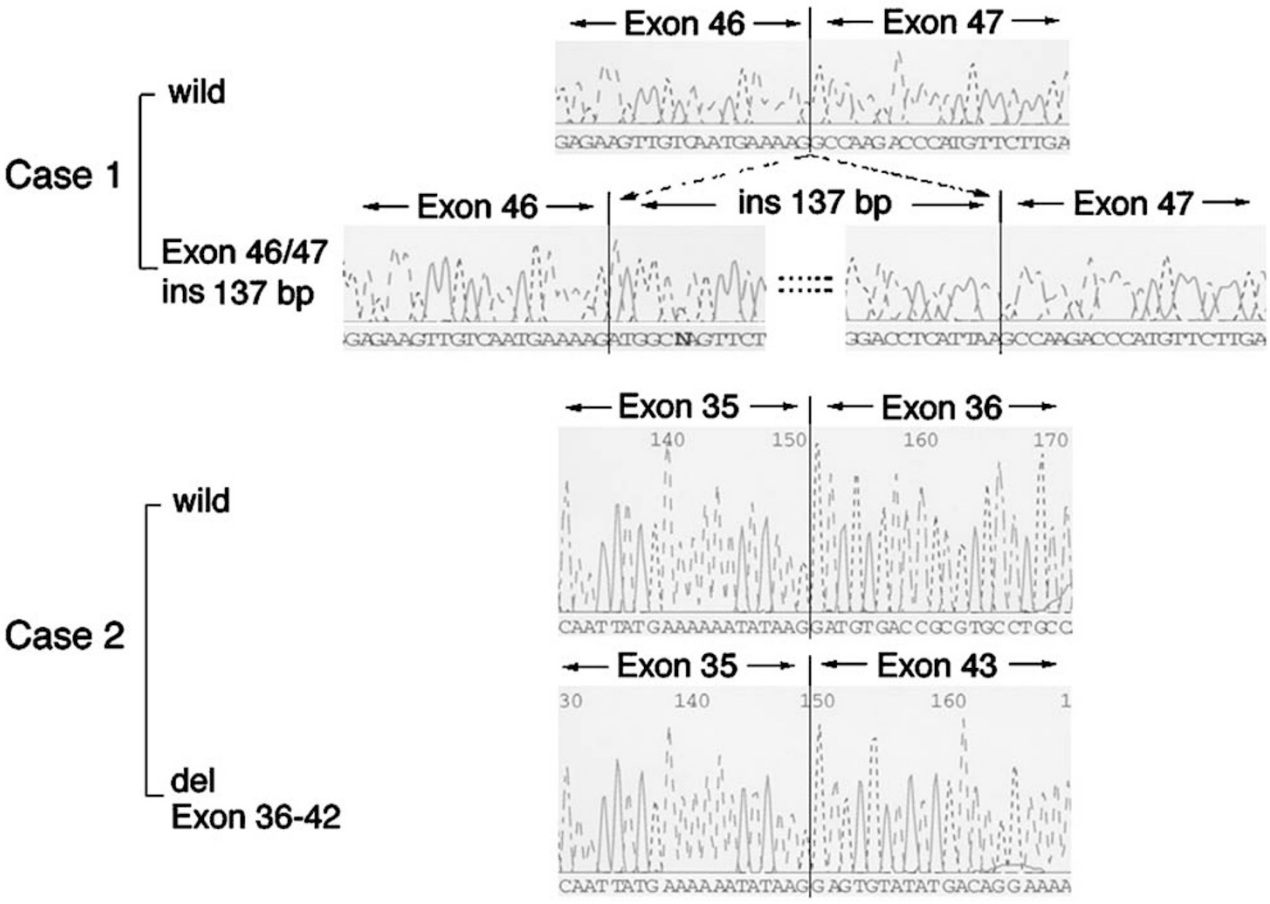

Figure 1 *ATR* gene mutations detected in clinical samples with PAL. Insertion of 137 bp from intron 46 between exons 46 and 47, the same mutation observed in OPL-2 line (Case 1), and deletion from nucleotides 6184–7297 which correspond to exons 36–42 (Case 2) were detected.

Cell Cycle Regulation

To examine whether cell cycle regulation is maintained or disrupted in the cell lines carrying *ATR* mutations, cell cycle distributions in cells exposed to 2 Gy of IR and 10 J/m^2 of UV were analyzed by FCM (Figure 2). Cell cycle distributions in the cells that were exposed neither to IR nor UV were similar among five lines, showing high G1 and low G2 cells. After IR exposure, OPL-7 with wild type for *ATM* and *ATR* genes and IB4 cells had abundant G1 cells and fewer S cells, showing efficient G1–S arrest, while a decrease in G1 and increase in G2 phase were found in Pal-1 and OPL-2 cells with ATM and/or ATR mutations, indicating that these lines passed through G1–S phase and arrest at G2/M phase. AT(L)5KY cells also showed arrest at G2/M phase after exposure to IR.

After UV exposure, IB4 cells showed higher G1 and lower S cells than untreated control cells, indicating efficient G1–S arrest. In contrast, OPL-2 cells showed more decrease in G1 cells and increase in S cells than OPL-7, indicating the disruption of G1–S checkpoint after UV exposure. When compared to untreated control cells, Pal-1 line with UV exposure showed no significant change, indicating the loss of cell cycle regulation in any phase.

p53 Protein

Compared to unexposed cells, increased expression of p53 was found in OPL-7 and IB4 cells after IR and UV exposure (Figure 3). In contrast, expression level in OPL-2 slightly increased 4 h after IR exposure, but showed no obvious change after UV exposure, whereas p53 expression levels in Pal-1 cells did not change after IR exposure and rather decreased after UV exposure, indicating that IR and UV exposure did not induce p53 accumulation properly in OPL-2 and Pal-1 cells.

Repair of DNA DSBs Induced by IR

To evaluate whether *ATR* gene mutations result in impaired DNA DSBs repair, kinetics of DNA DSBs repair were examined using PFGE (Figure 4a). More than 80% of the DSBs in OPL-7 and IB4 lines were repaired within 1 h after IR exposure (Figure 4b). In contrast, about 75.3 and 69.2% of DSBs in OPL-2

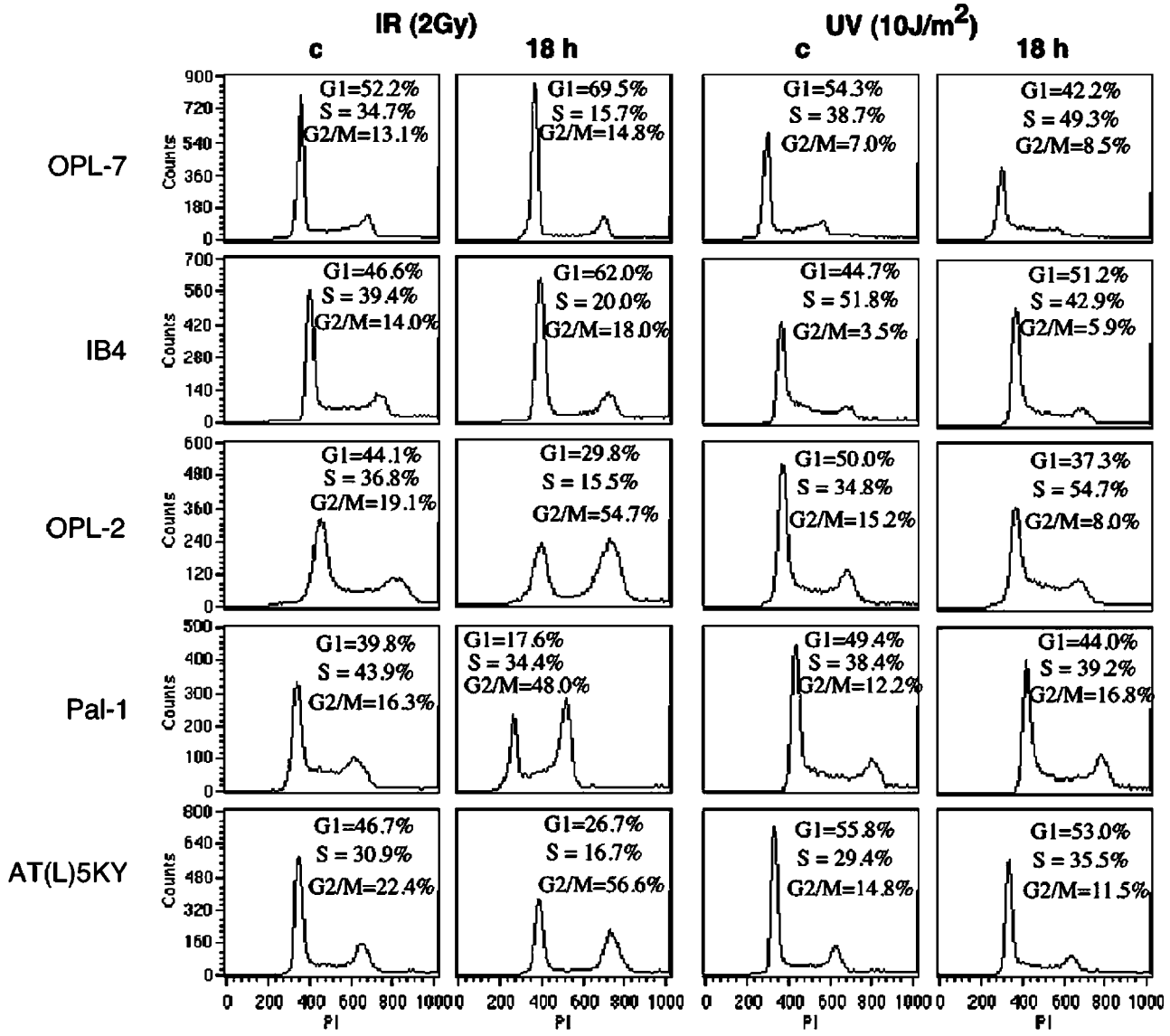

Figure 2 Cell cycle distribution in OPL-7, IB4, OPL-2, Pal-1, and AT(L)5KY lines after IR and UV exposure. Cells exposed to 2 Gy IR and 10 J/m^2 UV were incubated for 18 h at 37°C. DNA was stained by propidium iodide and analyzed by FCM. After IR exposure, OPL-2 and Pal-1 showed a decrease in G1 and an increase in G2 cells. After UV exposure, IB4 cells showed higher G1 and lower S cells than untreated control cells. OPL-2 cells showed a larger decrease in G1 cells and increase in S cells than OPL-7, whereas Pal-1 cells were not significantly different from untreated control cells.

and Pal-1 lines, respectively, remained unrepaired after 1 h, but mostly repaired after 6-h incubation. These results demonstrated that repair of DNA DSBs after IR exposure in OPL-2 and Pal-1 was delayed but not completely abrogated.

Repair of DNA SSBs Induced by UV

To evaluate whether mutations of *ATR* gene result in impaired DNA SSBs, OPL-2 and Pal-1 together with OPL-7, IB4, and AT(L)5KY cells were exposed to 10 J/m^2 of UV, and repair of DNA SSBs was evaluated by a Comet assay. After UV exposure, the comet tails were observed in all five cell lines, showing that DNA SSBs occurred (Figure 5a). The maximum DML was observed between 6- and 12-h incubation period in OPL-2, OPL-7, IB4, and AT(L)5KY cells (Figure 5b). Ratio of the DML at 18–6-h incubation periods after UV exposure was calculated, representing the ratio of unrepaired DNA SSBs (Figure 5c). In OPL-7 and IB4 cell lines, significant decrease in the DML was observed at 18 h after exposure. After 18-h incubation, a slight decrease of DML was observed in OPL-2 cells, whereas the DML of Pal-1 cells did not decrease after the 18-h incubation period. These results indicated that OPL-2 and Pal-1 line failed to repair DNA SSBs after UV exposure.

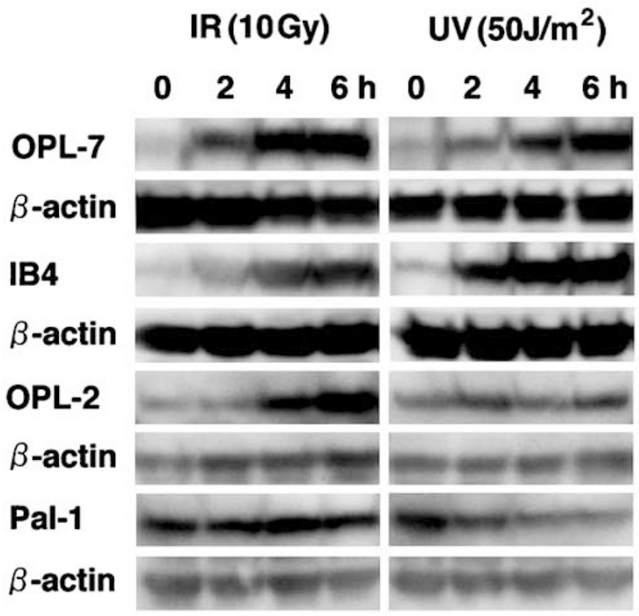

Figure 3 Accumulation of p53 protein. Equal numbers of cells were exposed to 10 Gy of IR and 50 J/m² of UV light, respectively, and incubated for up to 6 h. Whole cells were lysed and an equal volume of protein extracts were subjected to Western blot analysis using anti-p53 antibody. p53 protein accumulation in OPL-2 cells was delayed after IR exposure and abrogated after UV exposure. In Pal-1 cells, p53 was not activated following IR or UV exposure. In control cell lines, OPL-7 and IB4, p53 protein accumulated as expected after IR and UV exposure. Equivalence of loading of cell lysates is shown by anti-β-actin labeling.

Discussion

ATM gene mutations have been reported in numerous lymphoid malignancies: 46–67% of T-PLL,[13–15] 19–34% of B-CLL,[16–18] and 10–20% of diffuse large B-cell lymphoma (DLBL).[31,32] The present study revealed that heterozygous mutations of *ATM* were found in five (62.5%) of eight PAL lines that were derived from DLBL tissues, indicating that the frequency of *ATM* mutations was high in lymphoma developed in chronic inflammation. *ATM* contains the PI3K domain from codon 2656 to 3056, which harbors the catalytic site in the active kinase of PIKK family.[33] In all PAL lines but one, the mutations in *ATM* gene resulted in truncation or missense mutations involving the PI3K domain. Recent studies demonstrated that heterozygous mutations of *ATM* abrogated its function and thus might contribute to an increased risk for cancer development.[34] *ATM* mutations were detected in 33–67% of cells in the clones examined, whereas *ATM* transcripts could be amplified in three of five clinical samples, in which mutations could not be detected. *ATM* was not amplified at all in two cases. A possibility for occurrence of some abnormalities such as deletion, decrease or loss of expression of *ATM* gene could not be excluded, because analysis was confined to PI3K domain in these cases. The

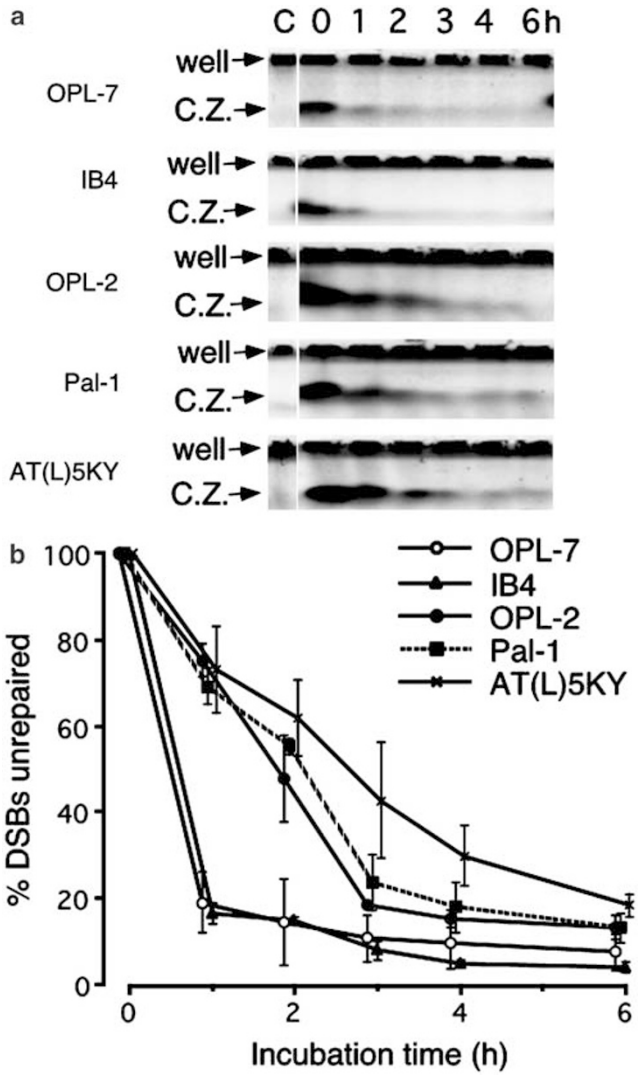

Figure 4 Induction and repair of DNA DSBs after IR exposure determined by PFGE. (**a**) Ethidium bromide-stained gel after PFGE. Equal numbers of OPL-7, IB4, OPL-2, Pal-1, and AT(L)5KY cells were embedded in 0.8% agarose plugs and exposed to 20 Gy IR. Cells were allowed to repair DSBs for 0–6 h at 37°C, then lysed to extracted DNA and subjected to PFGE. Untreated control is shown in the first lane. The upper bands derived from undamaged DNA or repaired DNA in wells. The lower bands show the compression zones (C.Zs) consisting of DSBs DNA. (**b**) Quantitation of DSB repair assays was performed. The percentage of unrepaired DSBs was calculated by ratio of signal from DSBs DNA in the C.Zs to DNA in the corresponding well. The percentage of unrepaired DSBs at 0-h incubation was set at 100%. Repair of DNA DSBs after IR exposure was delayed in OPL-2 and Pal-1 compared to control cell lines OPL-7 and IB4. The means (symbol) and standard deviation (error bar) from three experiments is depicted. Symbols represent cell lines: OPL-2 (●), Pal-1 (■), OPL-7 (○), IB4 (▲), AT(L)5KY (×).

present results suggested that *ATM* mutations might be involved in initiation and/or progression of PAL.

Information for the role of *ATR* gene alterations for lymphomagenesis has been limited until recently. *ATR* is an essential gene required for cell proliferation, therefore deletion of this gene causes early

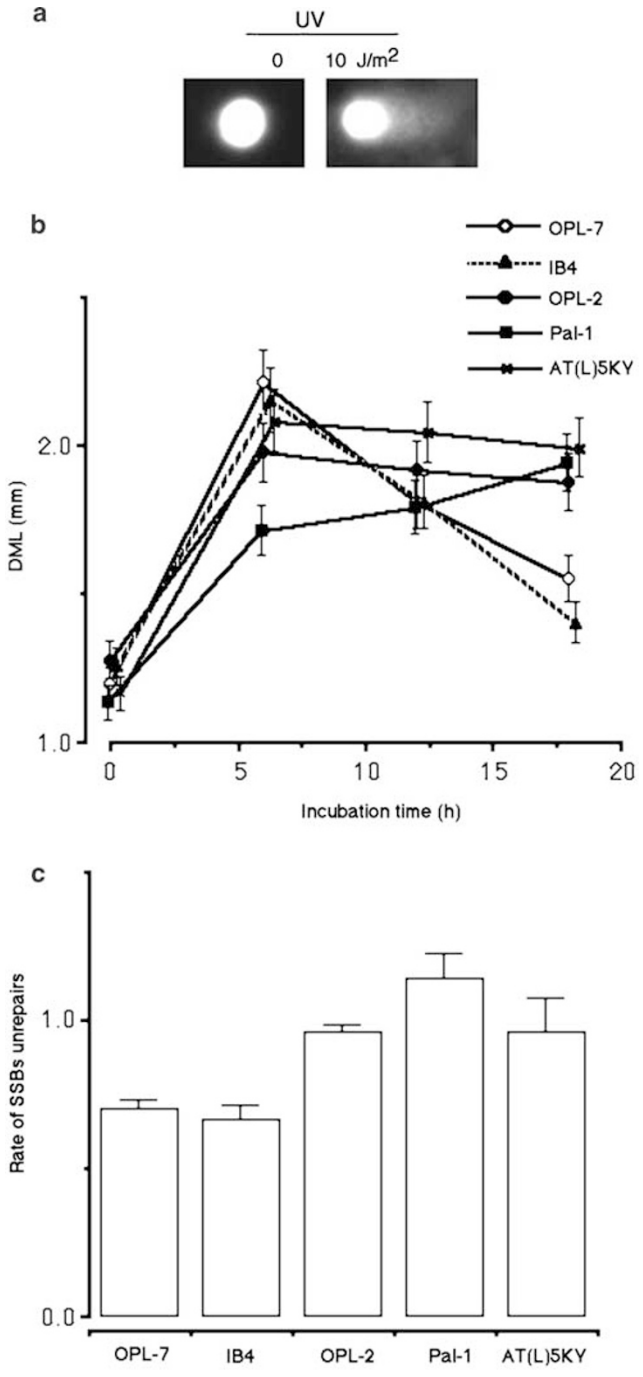

Figure 5 Repair of DNA SSBs after UV exposure determined by the Comet assay. (**a**) The representative pattern of cell DNA migration (comet tails) produced by the Comet assay. (**b**) OPL-7, IB4, OPL-2, Pal-1, and AT(L)5KY cells were exposed to 10 J/m^2 of UV, incubated at 37°C for 0–18 h, and assayed as described in Materials and methods. Compared to control cell lines OPL-7 and IB4, OPL-2 and Pal-1 showed failure and inability to repair DNA SSBs after UV exposure. The means (symbol) and standard deviation (error bar) from three experiments is depicted. Symbols represent cell lines: OPL-2 (●), Pal-1 (■), OPL-7 (○), IB4 (▲), AT(L)5KY (×). (**c**) Ratio of the DML at 18–6-h incubation after UV exposure, which represented the rate of unrepaired DNA SSBs. Rates in OPL-2 and Pal-1 cells were higher than those in OPL7 and IB4. DML indicates DNA migration length.

embryonic lethality.[19,20] Hematological malignancies may occur in patients with Seckel syndrome, in whom not only aberrant spliced transcript but also wild-type transcript of ATR are expressed, indicating that mutations of this gene may be involved in the pathogenesis of hematological malignancies in a dominant negative fashion.[23,35] Previous studies have also demonstrated that mice with heterozygous defects in *ATR* exhibit increased incidence of lymphoma.[19] In the present study, heterozygous frameshift and point mutations affecting the PI3K domain of *ATR*,[33] thus indicative of the loss-of-function mutation, were detected in two PAL lines. In the previous studies, shortening of poly A tracts within the sequence of *ATR* genes was described in sporadic stomach cancer with mutation of mismatch repair (MMR) genes,[36] whereas such a mutation was not observed in OPL-3, which is the only PAL line showing mismatch repair phenotype.[5] Further study is necessary to evaluate whether the mutation of *ATR* is frequent in lymphoid malignancies with mismatch repair phenotype or not.

Two cell lines with heterozygous mutations of *ATR* showed the abnormal response to DNA damage induced by IR and UV exposure. In normal cells, IR or UV exposure cause p53 activation and stabilization in response to DNA damage through activation of *ATM* and/or *ATR*, thus resulting in arrest at the G1–S checkpoint. However, a loss of G1–S arrest and impairment of p53 accumulation together with decreased ability of DNA repair were observed in OPL-2 and Pal-1 after IR or UV exposure. Pal-1 cells have fairly abundant p53 prior to irradiation, indicating aberrant expression of p53 in this line. DSB repair was delayed in both OPL-2 and Pal-1, while SSB repair was partially or completely abrogated in cells with *ATR* mutations (OPL-2) or both *ATM* and *ATR* mutations (Pal-1), respectively. These results were inconsistent with the well-known finding that activation of *ATM* is mainly triggered subsequent to DNA DSBs, while activation of *ATR* is induced by various forms of DNA damage and replication blocks, including UV-induced SSBs.[9–11,22] The present study raises the possibility that *ATR* mutations might be involved in the initiation and/or progression of PAL.

PAL develops in the pleural cavity affected by long-standing pyothorax resulted from artificial pneumothorax for the treatment of tuberculosis. In the chronically inflamed lesions, DNA damage might be induced by free radicals and oxidative stress. Antibacterial drugs and frequent X-ray examination for chronic pyothorax, from which PAL develops, might also cause DNA damage. Alterations of *ATM* and *ATR*, the responsive genes for DNA damage, might facilitate accumulation of chromosomal structural abnormalities as well as mutations of the genes. The present study clearly shows that alterations of *ATM* and *ATR* are frequent in PAL, suggesting a role of both *ATM* and *ATR* mutations for initiation and/or progression of PAL.

Acknowledgements

We thank Dr T Al Saati (Laboratoire d'Anatomie Pathologique CHU Purpan, France) for providing Deglis cell line, Dr GW Bornkamm (GSF-Research Center for Environment and Health, Munich, Germany) for BL36, BL60, BL137, Dr E Kieff (Brigham and Women's Hospital, Boston) for IB-4 and Drs M Matsuoka and Y Taniguchi (Kyoto University, Japan) for MT-1, MT-2, MT-4 cell lines, and Dr T Yamauchi (Fukui Medical University, Fukui, Japan) for valuable technical discussion. This work was also supported by grants from the Ministry of Education, Science, Culture, and Sports, Japan (14031213, 14770073, 15026209, 15406013, 15590340, 16390105).

References

1 Coussens LM, Werb Z. Inflammation and cancer. Nature 2002;420:860–867.
2 Nakatsuka S, Yao M, Hoshida Y, *et al.* Pyothorax-associated lymphoma: a review of 106 cases. J Clin Oncol 2002;20:4255–4260.
3 Iuchi K, Aozasa K, Yamamoto S, *et al.* Non-Hodgkin's lymphoma of the pleural cavity developing from long-standing pyothorax. Summary of clinical and pathological findings in thirty-seven cases. Jpn J Clin Oncol 1989;19:249–257.
4 Kanno H, Yasunaga Y, Ohsawa M, *et al.* Expression of Epstein–Barr virus latent infection genes and oncogenes in lymphoma cell lines derived from pyothorax-associated lymphoma. Int J Cancer 1996;67:86–94.
5 Takakuwa T, Luo WJ, Ham MF, *et al.* Establishment and characterization of unique cell lines derived from pyothorax-associated lymphoma which develops in long-standing pyothorax and is strongly associated with Epstein–Barr virus infection. Cancer Sci 2003; 94:858–863.
6 Daibata M, Taguchi T, Nemoto Y, *et al.* Epstein–Barr virus (EBV)-positive pyothorax-associated lymphoma (PAL): chromosomal integration of EBV in a novel CD2-positive PAL B-cell line. Br J Haematol 2001;117: 546–557.
7 Al Saati T, Delecluze HJ, Chittal S, *et al.* A novel human lymphoma cell line (Deglis) with dual B/T phenotype and gene rearrangements and containing Epstein–Barr virus genomes. Blood 1992;80:209–216.
8 Shiloh Y. ATM and related protein kinases: safeguarding genome integrity. Nat Rev Cancer 2003;3: 155–168.
9 Tibbetts RS, Cortez D, Brumbaugh KM, *et al.* Functional interactions between BRCA1 and the checkpoint kinase ATR during genotoxic stress. Genes Dev 2000; 14:2989–3002.
10 Zhou BB, Elledge SJ. The DNA damage response: putting checkpoints in perspective. Nature 2000;408: 433–439.
11 Khanna KK, Jackson SP. DNA double-strand breaks: signaling, repair and the cancer connection. Nat Genet 2001;27:247–254.
12 Rouse J, Jackson SP. Interfaces between the detection, signaling, and repair of DNA damage. Science 2002;297:547–551.
13 Stoppa LD, Soulier J, Lauge A, *et al.* Inactivation of the ATM gene in T-cell prolymphocytic leukemias. Blood 1998;91:3920–3926.
14 Stilgenbauer S, Schaffner C, Litterst A, *et al.* Biallelic mutations in the ATM gene in T-prolymphocytic leukemia. Nat Med 1997;3:1155–1159.
15 Vorechovsky I, Luo L, Dyer MJ, *et al.* Clustering of missense mutations in the ataxia-telangiectasia gene in a sporadic T-cell leukaemia. Nat Genet 1997; 17:96–99.
16 Bullrich F, Rasio D, Kitada S, *et al.* ATM mutations in B-cell chronic lymphocytic leukemia. Cancer Res 1999;59:24–27.
17 Starostik P, Manshouri T, O'Brien S, *et al.* Deficiency of the ATM protein expression defines an aggressive subgroup of B-cell chronic lymphocytic leukemia. Cancer Res 1998;58:4552–4557.
18 Schaffner C, Stilgenbauer S, Rappold GA, *et al.* Somatic ATM mutations indicate a pathogenic role of ATM in B-cell chronic lymphocytic leukemia. Blood 1999;94:748–753.
19 Brown EJ, Baltimore D. ATR disruption leads to chromosomal fragmentation and early embryonic lethality. Genes Dev 2000;14:397–402.
20 De Klein A, Muijtjens M, Van Os R, *et al.* Targeted disruption of the cell-cycle checkpoint gene ATR leads to early embryonic lethality in mice. Curr Biol 2000;10:479–482.
21 Brown EJ, Baltimore D. Essential and dispensable roles of ATR in cell cycle arrest and genome maintenance. Genes Dev 2003;17:615–628.
22 Cliby WA, Roberts CJ, Cimprich KA, *et al.* Overexpression of a kinase-inactive ATR protein causes sensitivity to DNA-damaging agents and defects in cell cycle checkpoints. EMBO J 1998;17:159–169.
23 O'Driscoll M, Ruiz PV, Woods CG, *et al.* A splicing mutation affecting expression of ataxia-telangiectasia and Rad3-related protein (ATR) results in Seckel syndrome. Nat Genet 2003;33:497–501.
24 Casper AM, Nghiem P, Arlt MF, *et al.* ATR regulates fragile site stability. Cell 2002;111:779–789.
25 Beamish H, Lavin MF. Radiosensitivity in ataxia-telangiectasia: anomalies in radiation-induced cell cycle delay. Int J Radiat Biol 1994;65:175–184.
26 Abbott DW, Freeman ML, Holt JT. Double-strand break repair deficiency and radiation sensitivity in BRCA2 mutant cancer cells. J Natl Cancer Inst 1998;90: 978–985.
27 Tice RR, Agurell E, Anderson D, *et al.* Single cell gel/comet assay: guidelines for *in vitro* and *in vivo* genetic toxicology testing. Environ Mol Mutagen 2000;35: 206–221.
28 Yamauchi T, Kawai Y, Ueda T. Enhanced DNA excision repair in CCRF-CEM cells resistant to 1,3-bis(2-chloroethyl)-1-nitrosourea, quantitated using the single cell gel electrophoresis (Comet) assay. Biochem Pharmacol 2003;66:939–946.
29 Cimprich KA, Shin TB, Keith CT, *et al.* cDNA cloning and gene mapping of a candidate human cell cycle checkpoint protein. Proc Natl Acad Sci USA 1996; 93:2850–2855.
30 Mannino JL, Kim W, Wernick M, *et al.* Evidence for alternate splicing within the mRNA transcript encoding the DNA damage response kinase ATR. Gene 2001;272:35–43.
31 Fang NY, Greiner TC, Weisenburger DD, *et al.* Oligonucleotide microarrays demonstrate the highest

frequency of ATM mutations in the mantle cell subtype of lymphoma. Proc Natl Acad Sci USA 2003;100:5372–5377.

32 Gronbaek K, Worm J, Ralfkiaer E, *et al.* ATM mutations are associated with inactivation of the ARF-TP53 tumor suppressor pathway in diffuse large B-cell lymphoma. Blood 2002;100:1430–1437.

33 Abraham RT. Cell cycle checkpoint signaling through the ATM and ATR kinases. Genes Dev 2001;15: 2177–2196.

34 Concannon P. ATM heterozygosity and cancer risk. Nat Genet 2002;32:89–90.

35 Wang P, Spielberger RT, Thangavelu M, *et al.* dic(5;17): a recurring abnormality in malignant myeloid disorders associated with mutations of TP53. Genes Chromosomes Cancer 1997;20:282–291.

36 Menoyo A, Alazzouzi H, Espin E, *et al.* Somatic mutations in the DNA damage-response genes ATR and CHK1 in sporadic stomach tumors with microsatellite instability. Cancer Res 2001;61:7727–7730.